Coded Fluid Antenna Multiple Access over Fast Fading Channels

Hanjiang Hong, Kai-Kit Wong, *Fellow, IEEE*, Kin-Fai Tong, *Fellow, IEEE*,
Hyundong Shin, *Fellow, IEEE*, and Yangyang Zhang

***Abstract*—Enabled by the emerging fluid antenna system (FAS) technology, fast fluid antenna multiple access (FAMA) provides a massive connectivity scheme which is able to serve on the same physical channel hundreds of users, without the need of precoding nor interference cancellation at each user. This is, however, only possible if we know the antenna position (i.e., port) in which the ratio of the instantaneous signal energy to the sum-interference plus noise signal energy is maximized on a per-symbol basis. In this letter, we address how fast FAMA can be approached using practical channel codes. This technique is referred to as coded FAMA. An iterative decoding receiver with a novel soft-decision port detector and the correlated demapper is proposed. Also, the average mutual information (AMI) for the coded FAMA system is derived to indicate the system's achievable transmission rate. Our results reveal that the spectral efficiency of the coded FAMA system can well approach the AMI with the proposed iterative decoding receiver. Moreover, it is illustrated that under rich scattering fast fading channels, the proposed coded FAMA system can support 120 users on the same channel to achieve a network spectral efficiency of 75 bps/Hz, without precoding.**

***Index Terms*—Fluid antenna, multiple access, coded modulation, iterative decoding, interference mitigation.**

I. Introduction

ONE KEY driver for the fifth generation (5G) and beyond systems is massive internet-of-things (IoT) [1], [2] which is very challenging to achieve due to the need of aggressive spectrum sharing and the inability to perform precoding with the sheer number of IoT devices. Contrary to the cellular setup, in which a base station (BS) is expected to adopt precoding to multiplex user signals in the spatial domain, the massive IoT scenarios are more complicated. Channel state information (CSI) at the transmitter side is often infeasible, and a multiple access technique that permits massive spectrum sharing and does not need transmitter CSI is highly desirable. Note that both non-orthogonal multiple access (NOMA) [3] and rate-splitting multiple access (RSMA) [4] are not suitable solutions either since they require CSI at the transmitter side for power allocation and user clustering. Furthermore, expecting an IoT device to perform successive interference cancellation (SIC) involving many interferers would be a tall order.

Motivated by the above, the aim of this letter is to develop a multiple access scheme that is capable of serving a massive number of users (i.e., IoT devices) on the same physical data channel, without the need of CSI at the transmitter side. The proposed scheme should also work on an interference channel in which the transmitters are distributed and not coordinated. To meet the aforesaid requirements, one emerging approach is fluid antenna multiple access (FAMA) [5], [6]. FAMA takes advantage of the antenna position flexibility enabled by the fluid antenna system (FAS) technology [7], [8], [9].

FAS was first proposed by Wong *et al.* in [10], [11]. Since then, there has been great interest in the performance of FAS in different channel models, e.g., [12], [13], [14], [15], [16], [17], [18]. Recent study in [19] also considered the multiple-input multiple-output (MIMO) FAS setup where FAS is installed at both ends. Channel estimation for FAS has also been tackled recently recognizing the spatial correlation [20], [21], [22].

For multiuser communications, FAMA exploits the unique feature of FAS to access the spatial opportunity in which the interference is weak. In [6], [23], it was proposed to switch to the position where the signal-to-interference plus noise ratio (SINR) is maximized. Recently, [24] presented an improved receiver architecture for FAS with the ability to handle more than 10 users. The schemes in [6], [23], [24] are referred to as *slow* FAMA since they only require each user's FAS to switch position once during each channel coherence time. By contrast, [5], [25] studied the *fast* FAMA scheme that switches position on a per-symbol basis. In so doing, the FAS can enjoy the position where the data-bearing sum interference plus noise signal cancels. FAMA is a receiver-centric approach that does not rely on precoding and interference is entirely dealt with by the FAS at each user. However, it is difficult to identify the best position on a per-symbol basis and [25] tried to address this problem. Nevertheless, it was shown that the multiple access ability reduced dramatically, partly because it cannot take full advantage of the "soft" detection in digital systems.

Motivated by this, this letter aims to reinstate the massive multiple access capability of FAMA by introducing the concept of *coded* FAMA. In particular, we employ the 5G New Radio (NR) encoder [26], [27] for the transmitters, and a soft-decision-based iterative decoding receiver is proposed for each user to leverage the potential of the coded FAMA system. In this receiver, we propose a soft-decision port detector to estimate the antenna ports and a correlated demapper using some or all ports in good condition. The soft-form log-likelihood ratio (LLR) is iteratively passed to the demapper, the decoder, and the port detector to improve better decoding performance. This soft-decision-based solution can compensate for channel effects and recover the error in the FAMA system. Finally, the average mutual information (AMI) of the coded FAMA system is derived to reveal the achievable rate, and guide the selection of the 5G modulation coding scheme (MCS).

II. The Coded FAMA System

In this letter, we consider a downlink channel[1] in which the BS communicates to U user terminals (UTs) each equipped

The work of K. Wong and K. Tong is supported by the Engineering and Physical Sciences Research Council (EPSRC) under Grant EP/W026813/1.

The work of H. Hong is supported in part by the Outstanding Doctoral Graduates Development Scholarship of Shanghai Jiao Tong University.

H. Hong, K. K. Wong and K. F. Tong are with the Department of Electronic and Electrical Engineering, University College London, London, United Kingdom. K. K. Wong is also affiliated with the Department of Electronic Engineering, Kyung Hee University, Yongin-si, Gyeonggi-do 17104, Korea.

H. Shin is affiliated with the Department of Electronic Engineering, Kyung Hee University, Yongin-si, Gyeonggi-do 17104, Korea.

Y. Zhang is with Kuang-Chi Science Limited, Hong Kong SAR, China.

Corresponding authors: K. K. Wong and H. Shin.

[1]Note that as CSI at the base station (BS) is assumed not available, the downlink model is equivalent to an interference channel.

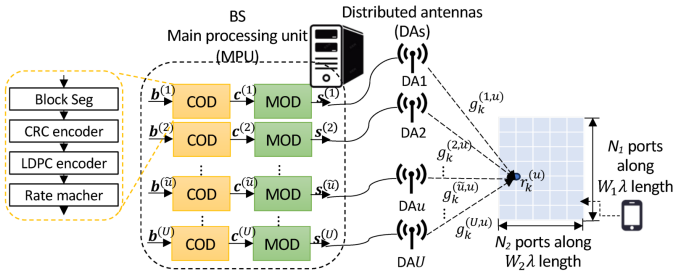

Fig. 1. System model of the coded FAMA system to a particular UT.

with a FAS. As shown in Fig. 1, the BS has U fixed-position distributed antennas (DAs) each responsible for sending an information-bearing signal to one designated UT. The information bit sequence $\mathbf{b}^{(u)}$ is encoded and then mapped to a symbol sequence $\mathbf{s}^{(u)}$. A 5G NR encoder is considered, including the block segmenter, the cyclic redundancy check (CRC) encoder, the low-density parity-check (LDPC) encoder, and the rate matcher. The detailed MCS is transmitted to the UT via the downlink control information in the physical downlink control channel (PDCCH) with negligible additional overhead.

At each UT, it is equipped with an N-port two-dimensional FAS (2D-FAS) with a physical size of $W_1\lambda \times W_2\lambda$, where λ is the wavelength. Over the 2D space, N_i ports are uniformly distributed along a linear space of length $W_i\lambda$ for $i \in \{1, 2\}$, so that $N = N_1 \times N_2$. For the sake of simplicity, we map the 2D antenna port indices to a single index $(k_1, k_2) \to k$, where $k_1 \in \{1, \ldots, N_1\}$, $k_2 \in \{1, \ldots, N_2\}$, and $k \in \{1, \ldots, N\}$. There are two main approaches for implementing fluid antennas. The first one uses a liquid-based solution [28] while the second adopts the reconfigurable pixel technology [29]. The latter is particularly suitable for delay-free port switching.

The received signal at the k-th port of UT u at time t is denoted by $r_k^{(u)}[t]$. Considering a fast fading channel $g_k^{(\tilde{u},u)}[t]$ from the $\tilde{u}$-th BS DA to the u-th UT, we have

$$r_k^{(u)}[t] = g_k^{(u,u)}[t]s^{(u)}[t] + \sum_{\substack{\tilde{u}=1 \\ \tilde{u}\neq u}}^{U} g_k^{(\tilde{u},u)}[t]s^{(\tilde{u})}[t] + \eta_k^{(u)}[t], \quad (1)$$

where $\eta_k^{(u)}[t]$ is the corresponding zero-mean complex Gaussian noise at time t, with the variance of σ_η^2.

A. Channel Model

The fast fading channels $\left\{g_k^{(\tilde{u},u)}[t]\right\}$ are correlated between the antenna ports k. Using the eigenvalue-based model [12], the channel $g_k^{(\tilde{u},u)}[t]$ can be expressed as

$$g_k^{(\tilde{u},u)}[t] = \sigma^{(\tilde{u},u)} \sum_{l=1}^{N} \sqrt{\lambda_l}\mu_{k,l} h_l^{(\tilde{u},u)}[t], \quad (2)$$

where $h_l^{(\tilde{u},u)}[t] \sim \mathcal{CN}(0, 1)$. In this letter, we simply set $\sigma^{(\tilde{u},u)} = \sigma, \forall \tilde{u}, u$. In the fast fading 2D-FAS channel, $h_l^{(\tilde{u},u)}[t]$ varies every symbol. For the sake of simplicity, the time index $[t]$ is omitted in the rest of the letter. In this case, the channel covariance matrix can be found as

$$\mathbb{E}\left[\mathbf{g}^{(\tilde{u},u)}\left(\mathbf{g}^{(\tilde{u},u)}\right)^{\dagger}\right] = \left(\sigma^{(\tilde{u},u)}\right)^2 \mathbf{\Sigma}, \quad (3)$$

where $\mathbf{g}^{(\tilde{u},u)} = [g_1^{(\tilde{u},u)}, \ldots, g_N^{(\tilde{u},u)}]^T$, the superscript T and $\dagger$ denote the transpose and hermitian operation, respectively, and the elements in $\mathbf{\Sigma}$ are given by [19]

$$[\mathbf{\Sigma}]_{k,l} = J_0\left(2\pi\sqrt{\left(\frac{k_1 - l_1}{N_1 - 1}W_1\right)^2 + \left(\frac{k_2 - l_2}{N_2 - 1}W_2\right)^2}\right), \quad (4)$$

where $(l_1, l_2) \to l$, and $J_0(\cdot)$ denotes the zero-order Bessel function of the first order. Singular value decomposition is carried out so that $\mathbf{\Sigma} = \mathbf{U}\mathbf{\Lambda}\mathbf{U}^{\dagger}$, where $\mathbf{\Lambda} = \mathrm{diag}\,(\lambda_1, \lambda_2, \ldots, \lambda_N)$, and $[\mathbf{U}]_{k,l} = \mu_{k,l}$. Notice that if $N_2 = 1$, the 2D-FAS channel falls into the one-dimensional FAS (1D-FAS) channel, and the spatial correlation is given by $[\mathbf{\Sigma}]_{k,l} = J_0\left(\frac{2\pi(k-l)W}{N-1}\right)$, where $W = W_1$, and $N = N_1$. Here, rich scattering is assumed.

B. Problem Statement

As in [25], we assume that UT u knows its channels $\mathbf{g}^{(u,u)}$ and the received signals $\mathbf{r}^{(u)} = [r_1^{(u)}, \ldots, r_N^{(u)}]^T$ instantly. Our objective is to find ways to utilize them so that reliable communication is possible in the case of massive access. In FAMA, each UT switches to the best port k^* for maxmizing the 'instantaneous' SINR [25], which requires the knowledge of the demapped symbol $\tilde{s}^{(u)}$ to calculate the instantaneous interference and noise $(\mathbf{r}^{(u)} - \mathbf{g}^{(u,u)}\tilde{s}^{(u)})$. In [25, (14)], a hard demapper for $\tilde{s}^{(u)}$ is proposed by minimizing the correlation between the channel and the interference, among which the 'cosine of angle' correlation scheme is demonstrated to preform best. Nevertheless, the hard-decision solutions lead to performance degradation in a coded system. Hence, our goal is to establish a soft-decision receiver for the coded-FAMA system, with the given $\left\{\mathbf{r}^{(u)}, \mathbf{g}^{(u,u)}, \chi, \sigma^2, \Sigma, \sigma_\eta^2\right\}$, where χ denotes the digital symbol constellation set.

III. Soft Coded FAMA Receiver

In this section, we propose a soft-decision iterative receiver to improve the reception performance of the coded FAMA system. As illustrated in Fig. 2, the proposed iterative decoder consists of the antenna port detector (P-DET), the correlated demapper (DEM), the deinterleaver (Π^{-1}), the interleaver (Π), and the decoder (DEC). Specifically, the probabilities of the reliablity of the antenna ports are detected by P-DET, and LLR is calculated and transferred between DEM and DEC.

At the initial process, the *a priori* $p(k; I)$ and $p(s; I)$ are assumed equally likely, i.e., $p(k; I) = 1/N$ and $p(s; I) = 1/M$ where M is the modulation order. From the second pass, the *extrinsic* information $L\,(c; O)$ (generating from the soft-input-soft-output DEC) is interleaved and feedback as the *a priori* information $L(b_i; I)$ to the P-DET and DEM. As a result, the *a priori* $p\,(s; I)$ is then calculated as

$$p\,(s; I) = \prod_{i=0}^{m-1} \frac{\exp\left[(1 - b_i)\,L(b_i; I)\right]}{1 + \exp L(b_i; I)}, \quad (5)$$

where $b_i \in \{0, 1\}$ denotes the i-th bit of the bit vector that is mapped to symbol $s \in \chi$, with $m = \log_2 M$.

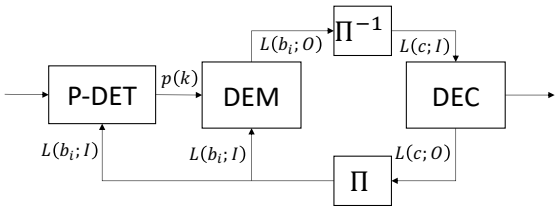

Fig. 2. The proposed iterative decoding receiver in the coded FAMA system.

Algorithm 1 P-DET

Require: $\mathbf{r}^{(u)}$, $\mathbf{g}^{(u,u)}$, $p(s;I)$, and $p(k;I)$;
Ensure: $p(k;O)$;
1: **for** $s \in \chi$ **do**
2: **for** $k = 1$ to N **do**
3: Calculate the PDF $p\left(\mathbf{r}^{(u)}|k^*=k,s\right)$ as (7);
4: **end for**
5: **end for**
6: **for** $k = 1$ to N **do**
7: Calculate the port probability $p\left(k;O\right)$ as (6);
8: **end for**

A. P-DET

A soft P-DET plays an important role to reveal the inherent channel states of the antenna ports. The proposed soft-decision port detector calculates the probability of the k-th port being the best port. As a result, the *a posteriori* probability $p\left(k;O\right)$ can be calculated as

$$\begin{aligned} p\left(k;O\right) &= \frac{\sum_{s\in\chi} p\left(k^*=k|s,\mathbf{r}^{(u)}\right) p\left(s;I\right)}{p\left(k;I\right)} \\ &= \frac{\sum_{s\in\chi} p(\mathbf{r}^{(u)}|k^*=k,s) p\left(s;I\right)}{\sum_{\tilde{k}=1}^{N} p(\mathbf{r}^{(u)}|k^*=\tilde{k},s) p(\tilde{k};I)}, \end{aligned} \tag{6}$$

in which $\mathbf{r}^{(u)} = [r_1^{(u)}, \ldots, r_N^{(u)}]^T$ denotes the received signal vector, and the conditional probability density function (PDF) $p\left(\mathbf{r}^{(u)}|k^*=k,s\right)$ is calculated as

$$p\left(\mathbf{r}^{(u)}|k^*=k,s\right) = \frac{1}{\pi\hat{N}} \exp\left(-\frac{|r_k^{(u)} - g_k^{(u,u)} s|^2}{\hat{N}}\right), \tag{7}$$

where $\hat{N} = (U-1)E_s\sigma^2 + \sigma_\eta^2$ is the average interference and noise power, and $E_s = \mathbb{E}[|s|^2]$ is the average signal power. The proposed P-DET is detailed in Algorithm 1.

With the output probabilities of the P-DET, we can sort the ports and select the antenna ports with higher probabilities for subsequent processing. We set a threshold p_{th} and choose the antenna ports with probabilities higher than p_{th}. That is, the received signal vector $\mathbf{r}^* = [\mathbf{r}^{(u)}]_{p(k)>p_{\text{th}}}$ and the channel vector $\mathbf{g}^* = [\mathbf{g}^{(u,u)}]_{p(k)>p_{\text{th}}}$ with dimension N^* are employed in the correlated demapper (DEM), with the UT index omitted. When the threshold p_{th} increases, more ports are considered for demapping, and the demapper will be more accurate with increasing complexity. There is a trade-off between accuracy and complexity depending on p_{th}. The threshold p_{th} should be decided according to practicality considering this trade-off.

B. DEM

Signals from the selected ports ($p(k) > p_{\text{th}}$) are utilized at the demapper. Considering the correlated channels of FAS, we propose a correlated demapper (DEM) to calculate the soft information of each bit in LLR form. The *extrinsic* LLR with Log-MAP demapping of the i-th bit $L(b_i;O)$ is given by

$$L\left(b_i;O\right) = \ln \frac{\sum_{s\in\chi_i^{(0)}} p\left(\mathbf{r}^*|s\right) p\left(s;I\right)}{\sum_{s\in\chi_i^{(1)}} p\left(\mathbf{r}^*|s\right) p\left(s;I\right)} - L\left(b_i;I\right), \tag{8}$$

where $\chi_i^{(b)}$ denotes the constellation subset with the i-th bit being $b \in \{0,1\}$. The conditional PDF $p\left(\mathbf{r}^*|s\right)$ in (8) over the correlated FAS channel is calculated as

$$p\left(\mathbf{r}^*|s\right) = \frac{1}{\pi^{N^*}|\hat{\mathbf{\Sigma}}^*|} \exp\left[-\left(\mathbf{r}^* - \mathbf{g}^* s\right)^\dagger \hat{\mathbf{\Sigma}}^* \left(\mathbf{r}^* - \mathbf{g}^* s\right)\right], \tag{9}$$

where $\hat{\mathbf{\Sigma}}^* = [\hat{\mathbf{\Sigma}}]_{p(k)>p_{\text{th}}}$ denotes the covariance matrix of the selected ports, and $\hat{\mathbf{\Sigma}} = (U-1)E_s\sigma^2\mathbf{\Sigma} + \sigma_\eta^2\mathbf{I}$.

The demapping complexity of DEM is $\mathcal{O}\left(M \times (N^*)^2\right)$, depending on the number of multiplication operations in the PDF calculation (9). The complexity decreases while the probability threshold p_{th} increases, but it may lead to performance degradation. If $p_{\text{th}} = 0$, all the antenna ports are utilized in the demapper, and the complexity will be $\mathcal{O}\left(M \times N^2\right)$.

C. AMI and MCS Selection

The achievable rate of the coded FAMA system can be measured by AMI [30], a.k.a. the bit-interleaved coded modulation (BICM) capacity. The AMI for each UT of the coded FAMA system is calculated as

$$C_B = m + \sum_{i=0}^{m-1} \mathbb{E}_{b,\mathbf{r}}\left[\log_2 \frac{\sum_{s\in\chi_i^{(b)}} p\left(\mathbf{r}|s\right)}{\sum_{s\in\chi} p\left(\mathbf{r}|s\right)}\right], \tag{10}$$

where the conditional PDF $p\left(\mathbf{r}|s\right)$ is calculated as the correlated conditional PDF (9) by setting $p_{\text{th}} = 0$ and $\mathbf{r} = \mathbf{r}^{(u)}$.

To ensure error-free transmission, the AMI C_B (in bit/s/Hz) has to be larger than the transmission rate, i.e., $m \times R < C_B$, where R denotes the code rate. Hence, the MCS selection has to follow this guideline with a specific FAS configuration.

IV. Simulation Results

This section presents the simulation results to evaluate the performance of coded FAMA with the proposed FAS receiver. The encoder (ENC) of the coded FAMA system is based on the 5G NR encoder [26]. The simulation bandwidth is 1.4 MHz, the available bandwidth is 1.08 MHz, the subcarrier spacing is $\Delta f = 15$ kHz, the number of subcarriers in a physical resource block is $N_{\text{sc}}^{\text{RB}} = 12$, and the number of resource elements is $N_{\text{RE}} = 936$. We use the 5G NR MCSs defined in [27, Table 5.1.3.1-1]. The channel model is described in (2).

The results in Fig. 3 are provided for the AMI per UT using Monte-Carlo simulations against the number of UTs U. The modulation constellation is quadrature amplitude modulation (QAM) with modulation order $M = 16$ (16QAM). It can be seen that the AMI of each UT decreases with the number of UTs, meaning that a robust MCS is desired for the system

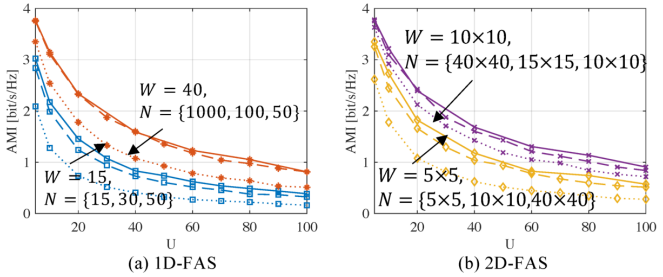

Fig. 3. AMI of a typical UT against the number of UTs U in the coded FAMA system for 16QAM.

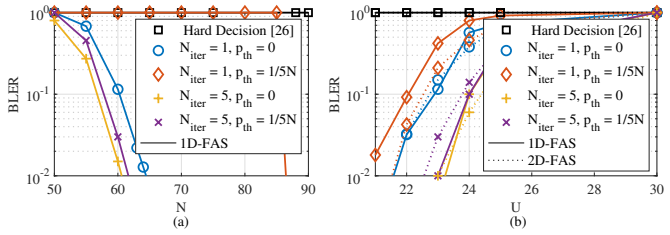

Fig. 4. BLER performance of the coded FAMA system against (a) the number of ports N, and (b) the number of UTs U.

with a large number of UTs. With a fixed physical size W, increasing N helps improve the AMI if N is small, but the gain diminishes when N is sufficiently large due to the strong correlation. Moreover, as expected, the AMI improves with a larger physical size, and 2D-FAS can provide a similar AMI in a more reasonable size compared with 1D-FAS. For instance, the AMI of 2D-FAS with $W = 10 \times 10$ is similar to that of 1D-FAS with $W = 40$, if the number of ports is large.

Fig. 4 presents the block error rate (BLER) performances of the coded FAMA system. 5G NR MCS 13 with the target code rate of $490/1024$ and 16QAM modulation are used in this case. Fig. 4(a) presents the BLER results against the number of antenna ports N with $U = 16$ UTs and 1D-FAS with $W = 40$ while Fig. 4(b) addresses how the performance changes with the number of UTs, U, considering both 1D- and 2D-FAS configurations. For the 1D-FAS, we have $N = 100$ and $W = 40$, while for the 2D-FAS, we set $N = 15 \times 15$ and $W = 10 \times 10$ at each UT. The performance of the hard decision method using the *cosine-of-angle* demapper [25] and hard-input-hard-output decoder is also presented for comparison.

It can be observed that the proposed soft-decision receiver outperforms the hard decision method. The BLER performance of the iterative receiver with iteration times $N_{\text{iter}} = 5$ is better than that of non-iteration ($N_{\text{iter}} = 1$). With the fixed number of UTs, the iterative receiver requires less number of antenna ports. With fixed configuration of FAS, the iterative decoding receiver can support more UTs for error-free transmission. Moreover, comparing the results of different p_{th}, the performance of utilizing all the antenna ports (where $p_{\text{th}} = 0$) is better than setting a non-zero threshold. In Fig. 4(a), the performance degradation of the non-zero threshold compared to the zero threshold is huge in the non-iteration case, but the performance degradation will reduce in the iteration case. This is partly because iterative decoding can converge to optimal

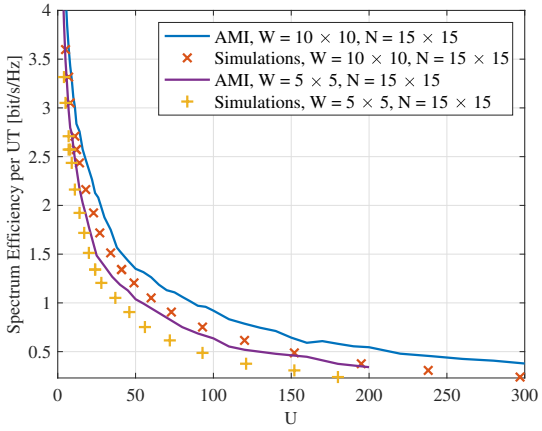

Fig. 5. Spectrum efficiency of each UT against the supported number of UTs with the iterative decoding receiver.

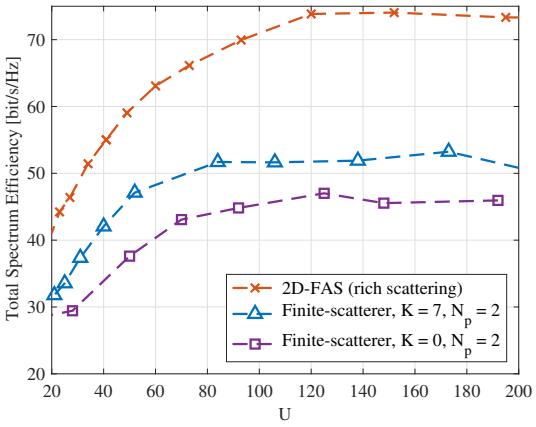

Fig. 6. Total spectrum efficiency against the supported number of UTs over the finite-scattering channel model.

decoding even with fewer ports involved. The degradation is also shown to be insignificant against the user number in Fig. 4(b), which means that a non-zero p_{th} could be considered to reduce the complexity when the number of antenna ports N is large for a fixed physical size W. Last but not least, the results in Fig. 4(b) also show that the performance of 1D-FAS with $W = 40$, $N = 100$ is similar to that of 2D-FAS with $W = 10 \times 10$, $N = 15 \times 15$.

The spectrum efficiency of the coded FAMA system with the iterative decoding receiver is then presented in Fig. 5. The same configuration as before is considered. All the ports are utilized (i.e., $p_{\text{th}} = 0$), and we set the iterative times as $N_{\text{iter}} = 5$. The spectrum efficiency is calculated as $\text{SE} = \text{TBS}/N_{\text{RE}} = R \times m$, where TBS refers to the transport block size specified in 5G NR. The criterion is to select the largest U that provides a BLER lower than 10^{-2} at each MCS, and plot the spectrum efficiency against U at this MCS. The AMIs are plotted for comparison. We employ 64QAM for low UT numbers ($U \leq 12$ for $W = 10 \times 10$, and $U \leq 8$ for $W = 5 \times 5$), 16QAM for medium UT numbers ($12 < U \leq 40$ for $W = 10 \times 10$, and $8 < U \leq 20$ for $W = 5 \times 5$), and quadrature phase shift keying (QPSK) for high UT numbers ($U > 40$ for $W = 10 \times 10$, and $U > 20$ for $W = 5 \times 5$). The simulation results approach

the theoretical AMI values, which prove the MCS selection strategy in Section III-C. With $N = 15 \times 15$ ports over the physical size $10\lambda \times 10\lambda$ FAS configuration, the system can support low error transmission for 8 UTs via MCS 19 at the transmission rate of 3.03 bit/s/Hz, for 60 UTs via MCS 7 at the rate of 1.03 bit/s/Hz, and for 152 UTs via MCS 3 at the rate of 0.49 bit/s/Hz. The rightmost simulation points show that the system can support 180 and 297 UTs with $W = 5 \times 5$ and $W = 10 \times 10$, respectively, via MCS 0 with the smallest rate of 0.24 bit/s/Hz. The results demonstrate that the coded FAMA system can support error-free transmission of hundreds of UTs at a low transmission rate, crucial to massive IoT.

Finally, we examine the performance of coded FAMA under the finite-scatterer channel model [31]. In Fig. 6, we present the simulation results of the total spectrum efficiency against the number of UTs, where the total spectrum efficiency is calculated as SE $\times U$. A 2D-FAS configuration of $N = 15 \times 15$ and $W = 10 \times 10$ is considered. When U is small, the total spectrum efficiency increases with the number of UTs. However, it tends to saturate as expected when U becomes too large to deal with. Moreover, the performance of the finite-scatterer channel is a bit worse than that of the rich scattering channel, partly because the proposed demapper is specifically designed for the rich scattering channel. With that being said, the coded FAMA system can still support approximately 40 UTs at the rate of 1.03 bit/s/Hz, and more than 100 UTs at the rate of 0.5 bit/s/Hz with the Rice factor $K = 7$ and the number of scattered components $N_p = 2$.

V. Conclusion

In this letter, we proposed the coded FAMA system with an iterating decoder to exploit the channels of FAS for massive access. At each UT, a soft-decision antenna port detector was proposed to evaluate the confidence level of any port being the best port. Correlated demapper (DEM) and iterative decoder were adopted to improve the overall performance of the coded FAMA system. Our simulation results demonstrated that more than 100 UTs could be supported on the same physical data channel to achieve over 70 bit/s/Hz utilizing coded FAMA without the need of precoding or any optimization from the transmitter side. This transmitter CSI-free approach highlights the enormous potential of coded FAMA for future wireless communications exploiting the unique advantages of FAS. A well-designed coding and modulation scheme is expected to further enhance the capability of the coded FAMA system and it would be interesting to explore the coding and modulation design explicitly tailored for the coded FAMA system.

References

[1] L. Chettri and R. Bera, "A comprehensive survey on Internet of Things (IoT) toward 5G wireless systems," *IEEE Internet Things J.*, vol. 7, no. 1, pp. 16–32, Jan. 2020.

[2] X. Chen *et al.*, "Massive access for 5G and beyond," *IEEE J. Select. Areas Commun.*, vol. 39, no. 3, pp. 615–637, Mar. 2021.

[3] M. Shirvanimoghaddam, M. Dohler and S. J. Johnson, "Massive non-orthogonal multiple access for cellular IoT: Potentials and limitations," *IEEE Commun. Mag.*, vol. 55, no. 9, pp. 55–61, Sept. 2017.

[4] Y. Mao *et al.*, "Rate-splitting multiple access: Fundamentals, survey, and future research trends," *IEEE Commun. Surv. & Tut.*, vol. 24, no. 4, pp. 2073–2126, Fourthquarter 2022.

[5] K. K. Wong and K. F. Tong, "Fluid antenna multiple access," *IEEE Trans. Wireless Commun.*, vol. 21, no. 7, pp. 4801–4815, Jul. 2022.

[6] K. K. Wong, *et al.*, "Slow fluid antenna multiple access," *IEEE Trans. Commun.*, vol. 71, no. 5, pp. 2831–2846, May 2023.

[7] K. K. Wong, K. F. Tong, *et al.*, "Bruce Lee-inspired fluid antenna system: Six research topics and the potentials for 6G," *Frontiers Commun. and Netw., section Wireless Commun.*, vol. 3, no. 853416, Mar. 2022.

[8] K. K. Wong, *et al.*, "Fluid antenna system–Part I: Preliminaries," *IEEE Commun. Lett.*, vol. 27, no. 8, pp. 1919–1923, Aug. 2023.

[9] C. Wang *et al.*, "AI-empowered fluid antenna systems: Opportunities, challenges, and future directions," to appear in *IEEE Wireless Communications*, 2024.

[10] K. K. Wong, K. F. Tong, Y. Zhang, *et al.*, "Fluid antenna system for 6G: When Bruce Lee inspires wireless communications," *Elect. Lett.*, vol. 56, no. 24, pp. 1288–1290, Nov. 2020.

[11] K. K. Wong *et al.*, "Fluid antenna systems," *IEEE Trans. Wireless Commun.*, vol. 20, no. 3, pp. 1950–1962, Mar. 2021.

[12] M. Khammassi, A. Kammoun and M.-S. Alouini, "A new analytical approximation of the fluid antenna system channel," *IEEE Trans. Wireless Commun.*, vol. 22, no. 12, pp. 8843–8858, Dec. 2023.

[13] W. K. New, K. K. Wong, H. Xu, K. F. Tong and C.-B. Chae, "Fluid antenna system: New insights on outage probability and diversity gain," *IEEE Trans. Wireless Commun.*, vol. 23, no. 1, pp. 128–140, Jan. 2024.

[14] J. D. Vega-Sánchez, A. E. López-Ramírez, L. Urquiza-Aguiar, *et al.*, "Novel expressions for the outage probability and diversity gains in fluid antenna system," *IEEE Wireless Commun. Lett.*, vol. 13, no. 2, pp. 372–376, Feb. 2024.

[15] J. D. Vega-Sánchez, L. Urquiza-Aguiar, M. C. P. Paredes, *et al.*, "A simple method for the performance analysis of fluid antenna systems under correlated Nakagami-m fading," *IEEE Wireless Commun. Lett.*, vol. 13, no. 2, pp. 377–381, Feb. 2024.

[16] P. D. Alvim *et al.*, "On the performance of fluid antennas systems under α-μ fading channels," *IEEE Wireless Commun. Lett.*, vol. 13, no. 1, pp. 108–112, Jan. 2024.

[17] C. Psomas, P. J. Smith, H. A. Suraweera, *et al.*, "Continuous fluid antenna systems: Modeling and analysis," *IEEE Commun. Lett.*, vol. 27, no. 12, pp. 3370–3374, Dec. 2023.

[18] Xu, Hao, *et al.*."Capacity maximization for FAS-assisted multiple access channels," *arXiv preprint*, arXiv:2311.11037, Nov. 2023.

[19] W. K. New, K.-K. Wong, *et al.*, "An information-theoretic characterization of MIMO-FAS: Optimization, diversity-multiplexing tradeoff and q-outage capacity," *IEEE Trans. Wireless Commun.*, vol. 23, no. 6, pp. 5541–5556, Jun. 2024.

[20] C. Skouroumounis and I. Krikidis, "Fluid antenna with linear MMSE channel estimation for large-scale cellular networks," *IEEE Trans. Commun.*, vol. 71, no. 2, pp. 1112–1125, Feb. 2023.

[21] H. Xu *et al.*, "Channel estimation for FAS-assisted multiuser mmWave systems," *IEEE Commun. Lett.*, vol. 28, no. 3, pp. 632–636, Mar. 2024.

[22] Z. Zhang, J. Zhu, L. Dai, *et al.*, "Successive Bayesian reconstructor for channel estimation in fluid antenna systems," *arXiv preprint*, arXiv:2312.06551v3, 2024.

[23] H. Xu *et al.*, "Revisiting outage probability analysis for two-user fluid antenna multiple access system," *IEEE Trans. Wireless Commun.*, vol. 23, no. 8, pp. 9534-9548, Aug. 2024.

[24] K. K. Wong, C.-B. Chae, and K. F. Tong, "Compact ultra massive antenna array: A simple open-loop massive connectivity scheme," *IEEE Trans. Wireless Commun.*, vol. 23, no. 6, pp. 6279–6294, Jun. 2024.

[25] K. K. Wong, K. F. Tong, Y. Chen, *et al.*, "Fast fluid antenna multiple access enabling massive connectivity," *IEEE Commun. Lett.*, vol. 27, no. 2, pp. 711–715, Feb. 2023.

[26] "NR; Multiplexing and channel coding," Available [Online]: https://www.3gpp.org/ftp/Specs/archive/38_series/38.212/38212-i20.zip, Last Accessed on 2024-03-29.

[27] "NR; Physical layer procedures for data," Available [Online]: https://www.3gpp.org/ftp/Specs/archive/38_series/38.214/38214-i20.zip, Last Accessed on 2024-03-29.

[28] Y. Shen *et al.*, "Design and implementation of mmWave surface wave enabled fluid antennas and experimental results for fluid antenna multiple access," *arXiv preprint*, arXiv:2405.09663, May 2024.

[29] J. Zhang *et al.*, "A pixel-based reconfigurable antenna design for fluid antenna systems," *arXiv preprint*, arXiv:2406.05499, Jun. 2024.

[30] G. Caire, G. Taricco, and E. Biglieri, "Bit-interleaved coded modulation," *IEEE Trans. Inf. Theory*, vol. 44, no. 3, pp. 927–946, May 1998.

[31] S. Buzzi and C. D'Andrea, "On clustered statistical MIMO millimeter wave channel simulation," *arXiv preprint*, arXiv:1604.00648v2, May 2016.